Master's Thesis

Development of Empirical Model for Li-ion batteries and Application to Dynamic Aging Pattern

Hansu Cheon

School of Energy and Chemical Engineering

(Energy Engineering(Battery Science and Technology))

Ulsan National Institute of Science and Technology

2024

Development of Empirical Model for Li-ion batteries and Application to Dynamic Aging Pattern

Hansu Cheon

School of Energy and Chemical Engineering
(Energy Engineering(Battery Science and Technology))

Ulsan National Institute of Science and Technology

Development of Empirical Model for Li-ion batteries and Application to Dynamic Aging Pattern

A thesis/dissertation submitted to
Ulsan National Institute of Science and Technology
in partial fulfillment of the
requirements for the degree of
Master of Science

Hansu Cheon

06.12.2024 of submission

Approved by

Advisor

Prof. Yunseok Choi

Development of Empirical Model for Li-ion batteries and Application to Dynamic Aging Pattern

Hansu Cheon

This certifies that the thesis/dissertation of Hansu Cheon is approved.

06.12.2024 of submission

Advisor: Prof. Yunseok Choi

Prof. Youngsik Kim

Prof. Wang-Geun Lee

Abstract

Recently, with the commercialization of many products using lithium-ion batteries, including Electric Vehicles (EVs), there has been significant interest in the capacity loss of the battery. Consequently, numerous studies have been conducted to investigate this topic.

In this study, I aimed to estimate the capacity loss of the electric vehicle (EV) battery under various operating conditions. To achieve this, I integrated an empirical model for estimating capacity loss through modeling and a CAP method that connects models under different conditions. The validation will be conducted by estimating the state of the degraded battery in the form of a pattern that changes in various ways.

As a result, it was shown that high-accuracy capacity loss estimation is possible with a small amount of computational power. This can be achieved by substituting stress factors extracted from pattern aging data into the model. Based on this, cost-effective on-board State of Health (SOH) estimation is expected to be possible.

Contents

List of Figures

List of Tables

I. Introduction

1.1 Overview of the technical requirements for estimating state of the battery

As the global usage of lithium-ion batteries continues to rise [1], it has already established itself as an essential energy source for modern society and it is used in many places in our lives, such as mobile phones, tablet PCs, and laptops. Apple, based in the United States, is a representative company that produces these products. Apple's value is remarkable, considering the rapid growth it has experienced. In August 2018, Apple became the first American company to reach a market capitalization of $1 trillion, achieving this milestone in 42 years. Surpassing $2 trillion took only two years, and the next trillion was achieved in just 16.5 months. [2]

Electric vehicles (EVs) are also a field that uses a lot of lithium-ion batteries, which contribute significantly to their higher prices compared to traditional internal combustion engine vehicles. [3] Nowadays, customers who buy products equipped with lithium-ion batteries, as mentioned above, are also particularly attentive to battery specification. In the second-hand market, the state of a product's battery plays a crucial role in determining its resale value. Consequently, there is an increasing demand for techniques to evaluate the states of batteries in active use.

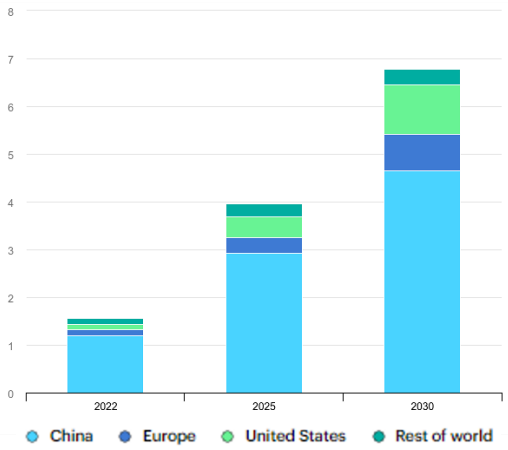

Figure 1. Growing Lithium-ion battery manufacturing capacity (TWh)

1.2 Understanding modeling the battery degradation

The capacity of lithium-ion batteries decreases due to various degradation mechanisms as it is used, [4] so nowadays, the estimation of SOH, which represents the state of the battery, is considered important and many methods have been studied. [5,6,7,8]

Generally, model-based estimators are expected to perform well, relying on an accurate battery model. In the model-based estimation framework, significant attention has been given to various estimation algorithms. [8] There are three main types of modeling methods for battery degradation: Electrochemical model, Equivalent Circuit Model (ECM) and Empirical model.

First, Electrochemical model is established for the purpose of describing the inner reactions inside the battery. It is in the form of a nonlinear Partial Differential Equation (PDE) and is based on the series of physical laws, such as Ohm's law, Faraday's first law and the Butler-Volmer equation. Typically, the parameters of an electrochemical model have their own physical description which allows for high accuracy. However, it is usually quite difficult to extract real parameters from electrochemical models. Therefore, when using electrochemical models, in addition to requiring knowledge of the electrochemical process, the computational burden must be considered.

Secondly, in the Equivalent Circuit Model (ECM), there are the abundant circuit components such as a voltage source related to State of Charge(SOC), an internal resistor, and Resistance-Capacitance networks, which provide researchers free to design a suitable structure for their applications. Among various ECM analysis methods, Electrochemical Impedance Spectroscopy (EIS) measurement is the most commonly used method. It is proposed through analyzing the Warburg element and describes the inherent electrochemical property of the battery. This method requires precise testing to obtain complex parameters, which can increase the cost of the equipment.

Third, Empirical model estimates degradation under corresponding conditions based on collected degradation data from reduced-order polynomial or mathematical expressions representing the essential characteristics of a battery. The Empirical model can estimate the degradation state of a

battery by substituting operating conditions such as current and temperature, which can be measured while using the battery, into an already constructed model. This makes it relatively simple to implement because there is no need to understanding the internal reaction of the battery or conduct precise tests to obtain parameters. However, to construct the initial model, a significant amount of data on charging and discharging for the battery is required, along with data under various operating conditions is for accuracy.

Modeling Methods	Empirical Model	Equivalent Circuit Model	Electrochemical Model
Modeling expression	$U_t = f(U_{oc}, SOC, I)$	$U_t = f(U_{oc}(SOC), I, R, C)$	$U_t = n \cdot f_{PDEs}$
Pros	Simple expression, computational efficiency	Easily understood, widely used in SOC estimation	High accuracy of voltage calculation
Cons	Limited capability of describing the terminal voltage	Complex parameter identification process	Require prior knowledge of the battery, time consuming

Table 2. Pros and cons of the modeling methods. [8]

In EVs, a field that typically uses lithium-ion batteries and requires condition diagnosis, the charging and discharging process of the battery does not maintain consistency like in the laboratory but changes rapidly under various conditions over time, as shown in Figure 2. For this reason, battery state estimation by charging and discharging in EVs must be done at a high speed. However, there are limits to the EV's computational power due to issues such as cost reductions of their manufacturer. Therefore, it can be said that an Empirical model that can estimate the state at low computational cost is more suitable for EV batteries than a complex Electrochemical model or ECM that requires high cost.

The evaluation of the performance or execution time of each model is typically presented in the form of a table in most papers. It is often compared using abstract language such as 'high', 'fast', and 'slow', making detailed quantitative comparison difficult. However, in the review paper by Jinhao Meng et al. [8], there is a table comparing the Mean Absolute Error (MAE) and execution time of some models, which I will cite for further explanation.

Model Type	MAE (V)	Execution Time (s)
Combined model	0.0212	6.3649×10^{-7}
Two RC ECM	0.0184	9.6155×10^{-7}
SPM	0.0159	2.2105×10^{-5}
SVM	0.0034	0.0018

Table 3. Comparison of the four models in MAE and execution time

The Combined model is a hybrid of an empirical model and an equivalent circuit model, combining the advantages of both models to estimate the voltage response of the battery. The Two RC ECM is a classic Equivalent Circuit Model and includes circuit components that describe the electrical characteristics of the battery. The Single Particle Model (SPM) is an electrochemical model that focuses on the electrochemical reactions occurring within the battery. Support Vector Machine (SVM) is a data-driven model that utilizes training data analysis to characterize battery performance.

To analyze the results, first of all, in terms of accuracy, SVM, which is a data-driven model, had the lowest error. However, this was attributed to the nature of the machine learning model because the training data and test data were the same in the paper, resulting in high accuracy. When they experimented again with different data, it was mentioned that the highest error of 0.0632 (V) of MAE was obtained. Therefore, in terms of accuracy excluding this, it can be said that the accuracy is high in the order of the electrochemical model SPM, two RC ECM, and the combined model of empirical model and ECM.

Secondly, in terms of execution time, among the remaining three models excluding SVM, SPM, a type of electrochemical model, was found to be about 300 to 400 times slower than the other two models. The combined model and ECM had similar execution times. However, since this execution time is significantly influenced by the computing device's performance, it can be considered as an to the approximate ratio reference.

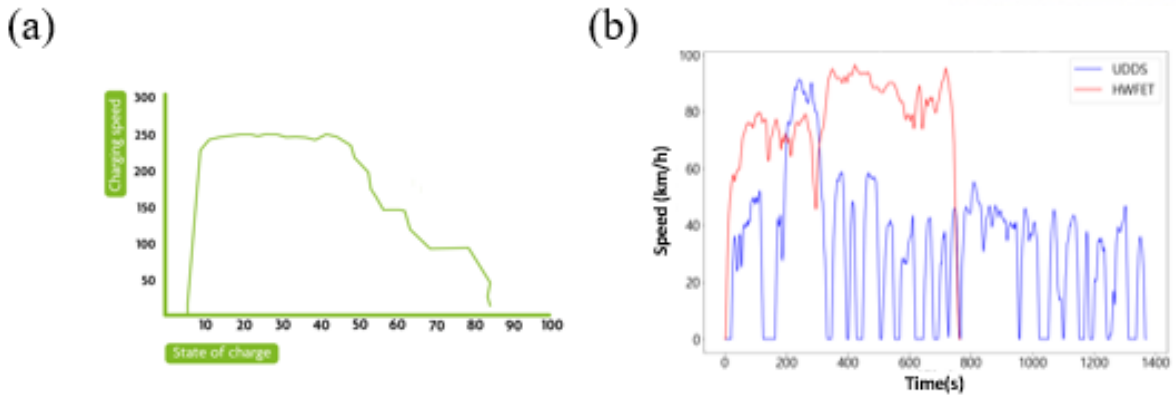

Figure 2. (a) Fast charging process of EVs and (b) Official driving schedule for testing EV mileage

In summary, by substituting the driving conditions extracted from the EV's battery data into an Empirical model, I will estimate the state of an EV battery that degrades under rapidly changing dynamic conditions.

II. Approach

2.1 Basic configuration of Empirical model

Empirical model is essentially based on mathematical relationships that link temperature, SOC, Ampere-hour throughput (AhTP) and SOC with internal resistance or capacity loss, depending on the discharge rate [7,8,9]. In numerous papers, a formula is created to expresses the degree of capacity loss for the stress factors specified by each author. The Empirical model is then established by fitting the coefficients through data obtained from experiments.

Based on this knowledge, I will explain the basic configuration of the Empirical model to be used in this study. The formula is shown in Figure 3.

(a)

$$Q_{loss} = f(\overleftrightarrow{X}) \cdot (AhTP)^{\alpha}$$

(b)

$$f(\overleftrightarrow{X}) = \beta_0 + \sum_i \beta_i X_i + \sum_{i \neq j} \beta_{ij} X_i X_j + \sum_i \beta_i X^2{}_i$$

$$\overleftrightarrow{X} = \sum_i X_i \,,\ Stress\ factors$$

$$\beta_i = Influence\ of\ factor\ X_i$$

Figure 3. (a) Formula of Empirical model and (b) Components of strength of stress

Figure 3 (a) represents the battery capacity loss Q_{loss} caused by the influence of various stress factors as a formula. It is the product of two terms: f(X), which represents the strength of stress, and the other one $AhTP^{\alpha}$, which represents the degree of stress accumulation through an increase in Ah throughput. To take a closer look at the f(X) term, which represents the strength of stress, as shown in Figure 3 (b), it is a quadratic polynomial consisting of the sum of the products of X and βs. X represents the stress

factor, such as charge or discharge current, SOC, and Depth of Discharge(DOD). βs represent the influence on the degradation of each factor. This was based on the Design of Experiments theory. [9]

Through experimental design, the main stress factors are first established. Data is collected through aging experiments, and the coefficients of the polynomial are obtained by substituting the amount of capacity decrease as AhTP increases and the exercise conditions for each set of data.

2.2 CAP method for connecting multiple models

In the previous chapter, I explained the framework of the Empirical model. By substituting each operating condition into the stress factor among the components in a well-constructed model using a sufficient amount of data, models corresponding to the conditions can be obtained. The amount of capacity loss can be estimated according to the increasing Ah throughput in the model.

However, since one Empirical model can only estimate capacity loss under one condition, to estimate battery capacity loss under dynamically changing conditions, not only are models corresponding to each condition required, but also a method of properly connecting each model is necessary.

Based on the literature research, there are two general methods to connect these models: CCT and CAP, both of which require the assumption of path independence [10]. The CCT (Cumulated Charge Throughput) method assumes that if two batteries are degraded under the same conditions at the same cycle, they will experience the same amount of capacity loss, regardless of the previous capacity state, as shown in Figure 4 (a). This method connects the models by vertically shifting the graphs, as illustrated in Figure 5 (a). On the other hand, the CAP (Current cAPacity) method assumes that if two batteries are degraded under the same conditions at the same capacity state, they will experience the same amount of capacity loss, regardless of the previous cycle, as shown in Figure 4 (b). This method connects the models by horizontally shifting the graphs, as depicted in Figure 5 (b).

In the paper introducing the two methods, the authors compare the accuracy of the CCT method and the CAP method for modeling capacity loss in lithium-ion batteries. They conclude that the CAP method estimates capacity loss with an accuracy of 2.5% to 6.7% more accurately compared to the CCT method, which has an accuracy of 7.5% to 18.8% for average cycling SOC change, DOD change, ambient temperature change, and discharge rate change. Therefore, this study adopts the CAP methodology.

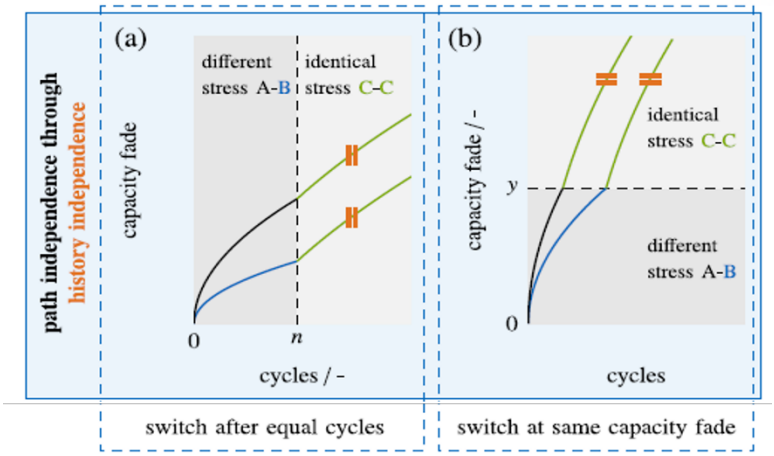

Figure 4. Two different definitions of path independence. (a)

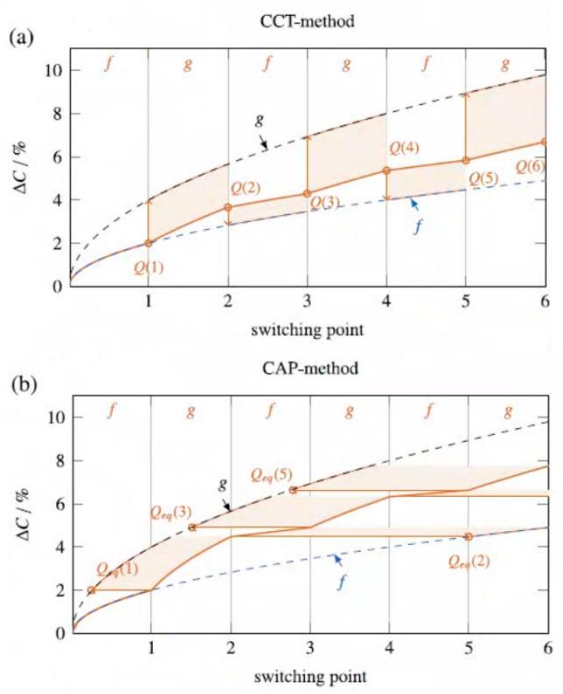

Figure 5. Visualization of the calculated capacity loss using the CCT method (a) and the CAP method (b) for 6 periodic switches between two cyclic capacity loss curves, f and g.

2.3 Three step plan for estimating the capacity loss of EV batteries

As mentioned in the Introduction, EV batteries degrade under various conditions, necessitating different capacity loss estimations for each condition, as illustrated in Figure 6. Therefore, this study's process to develop a method for estimating the battery state of EVs that degrade under dynamic conditions was summarized and presented in three steps.

First, determine the exponent α, which represents the degree of stress accumulation. This determines the shape of the model curve, which has the form of an exponential function, as shown in Figure 7. Second, determine the polynomial representing the strength of stress, detailed previously. This includes operating conditions set through experimental design, and the coefficients are determined by substituting data obtained through aging experiments. Finally, each model expressed as the product of the previous two terms is connected to each other according to the operating conditions extracted from the dynamic aging data to estimate the final capacity loss.

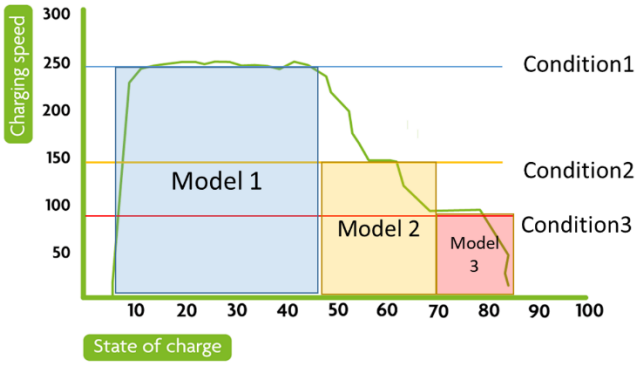

Figure 6. Different models for each condition

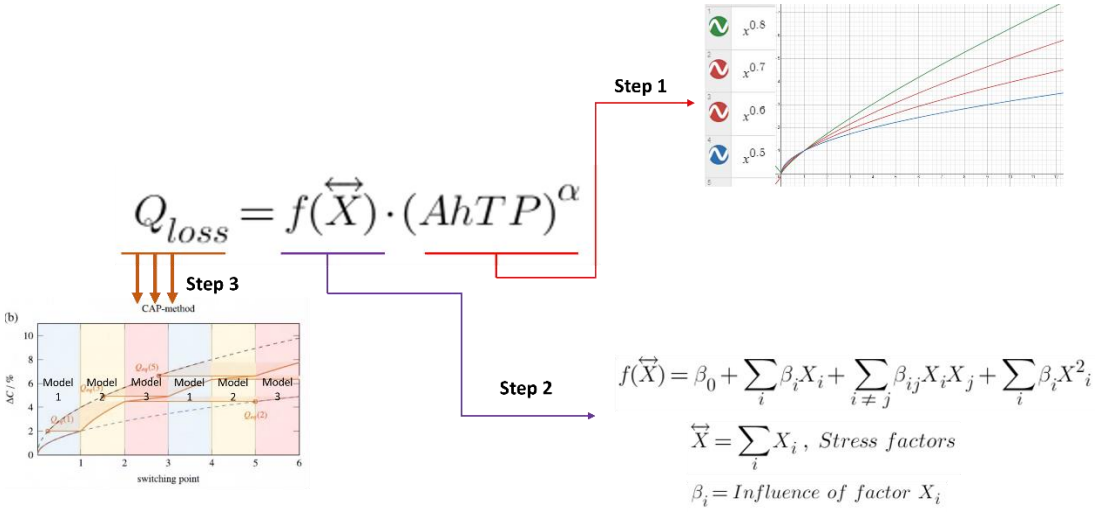

Figure 7. Summary of the method developed in this study

III. Experimental

3.1 Aging experiment

The aging experiments to obtain data for constructing the Empirical model were conducted using a SAMSUNG 50GB in the 21700 format, Nickel-Cobalt-Aluminum (NCA) cathode, and a Graphite-Silicon (Gr-Si) anode. The cell's detailed specifications are in Table 1 (a).

Since the main stress factors were defined as charge current, discharge current, State of Charge (SOC), and Depth of Discharge (DOD), the conditions of the experiment were set by controlling their changes. The experimental condition outline is in Table 1 (c): charge current was set to two levels - Low (0.3C, 1470mA) and High (0.8C, 3920mA), and the discharge current was also set to two levels - Low (0.5C, 2450mA) and High (1.0C, 4900mA). The SOC range was divided into three segments between 20% to 80%, resulting in three DOD values of 20% (20-40, 40-60, 60-80) and one of 60 (20-80). Since the charge and discharge at both ends (0-20, 80-100 range) of the SOC range have been reported to have a serious effect on the degradation of lithium-ion batteries [11,12], this condition was excluded from the design of experimental conditions to exclude unintended degradation. The experiment is not simply conducted from 0% to 100% SOC as in a general experiment. It is fully charged before cycling is started, and the capacity corresponding to the previous RPT capacity is discharged to set the SOC range. Then the charge and discharge of the capacity corresponding to the DOD are repeatedly performed. Detailed experimental process profiles are described in Table 1 (b). Additionally, a Reference Performance Test (RPT) was conducted before the start of the experiment and at the first 50, 100 cycles. After that, RPT was performed every 25 cycles. Three cells were tested for each aging condition to obtain data. In this experiment, RPT was composed of a capacity test consisting of a charge of 0.1C to minimize the effect of degradation, a normal discharge current of 0.2C, and a Hybrid Pulse Power Characterization (HPPC) test that extracts resistance parameters through pulse current in every 10% SOC section.

I controlled the experimental environment using a constant temperature and humidity control chamber

(Daesung E&T) and a cell cycler (Wonik PNE). The chamber was maintained at 25℃, simulating room temperature, and a temperature sensor was attached to each cell to measure its temperature during the experiment.

(a)

Manufacturer	Samsung SDI
Size	21700 (Cylindrical)
Nominal capacity	4900 mAh
Voltage range	2.5 ~ 4.2 V
Max charge current	1C (4900mA)
Max discharge current	2C (9800mA)

(b)

Temperature	Step	Mode	Condition	Cut-off
25℃	1	CCCV Charge	0.1C, 4.2V	>4.2V, <0.05C
	2	Rest	30min	
	3	CC Discharge	0.2C	Corresponding SOC
	4	Rest	30min	
Repeat 5-8	5	CCCV Charge	0.3C/0.8C	Corresponding SOC, >4.2V
	6	Rest	10min	
	7	CC Discharge	0.5C/1.0C	Corresponding SOC
	8	Rest	10min	

(c)

Discharge Current	Charge Current	DOD	Discharge Current	Charge Current	DOD
0.5C	0.3C	20~40	1C	0.3C	20~40
		40~60			40~60
		60~80			60~80
		20~80			20~80
	0.8C	20~40		0.8C	20~40
		40~60			40~60
		60~80			60~80
		20~80			20~80

Table 4. (a) Cell specification, (b) Cycle aging profile and (c) Experimental conditions.

3.2 Pattern aging experiments for validation

In order to validate that the Empirical model effectively diagnoses the battery status of the actual EV, data on the aged battery, such as the driving pattern of the EV, is required. Therefore, an aging schedule for verification was created using an ISO 12405-2 High-energy applications pattern [13] commonly used in the industry to simulate the driving pattern of EVs. Using this schedule, the same cells used in the aging experiment were degraded within the same SOC range of 20% to 80% to obtain data. Detailed experimental processes are outlined in Table 2.

As you can see from the table below, the charging and discharging process is repeated rapidly with currents of various C-rates (0.25C, 0.5C, 1.25C, 2.0C) within a few seconds within the pattern aging. The performance of the model, made with the empirical model manufactured through the data of the aging experiment conducted in 3.1, would be verified by estimating the state of the battery, which was degraded by this dynamic aging pattern.

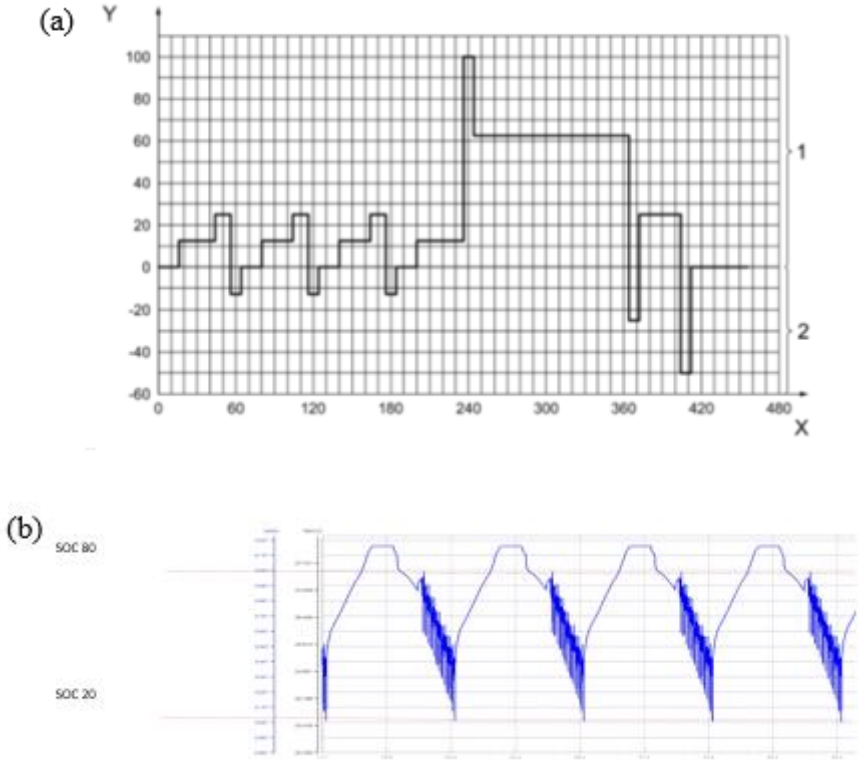

Figure 8. (a) ISO 12405-2 High-energy application pattern and (b) Pattern aging experiment

Step	Time increment [s]	Time cumulative [s]	Fraction of max. power [%]
1	16	16	0
2	28	44	+12,5
3	12	56	+25
4	8	64	−12,5
5	16	80	0
6	24	104	+12,5
7	12	116	+25
8	8	124	−12,5
9	16	140	0
10	24	164	+12,5
11	12	176	+25
12	8	184	−12,5
13	16	200	0
14	36	236	+12,5
15	8	244	+100
16	120	364	−62,5
17	8	372	−25
18	32	404	+25
19	8	412	−50
20	44	456	0

Table 5. Dynamic discharge power profile for the ISO 12405-2 pattern

3.3 Dataset preparation process

As mentioned earlier, a significant amount of data was needed to build the Empirical model. It took over 8 months to gather the data, and the capacity loss was monitored through RPT every 25cycles during aging for a total of 525 cycles. The SOC intervals were adjusted according to this capacity to regulate the experimental conditions.

All capacity losses occurred within a section above 80% SOH, commonly referred to as a linear degradation section. This section is where path independence is considered to be established in many papers [14,15].

The data visualizing the progress of the aging experiments is shown in Figure 3. Additionally, Table 3, summarizing the dataset overview is also presented.

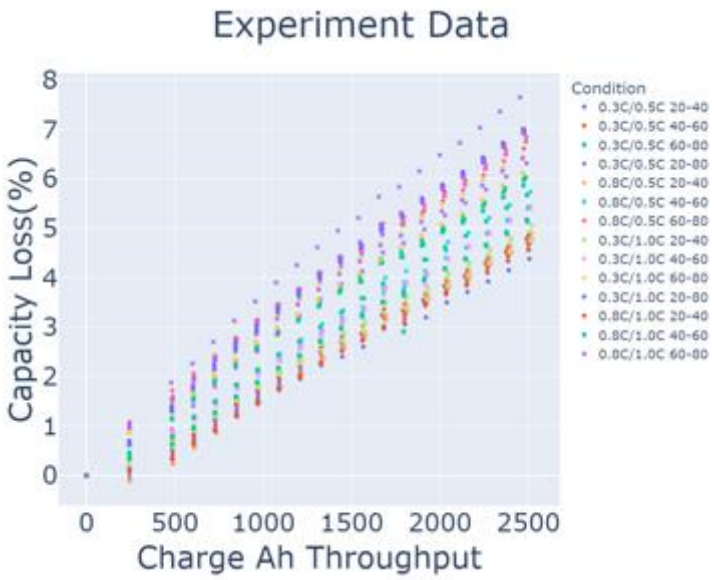

Figure 9. Visualized aging experimental process

Category	Value
Cycle(Schedule)	525
Average EFC	508.4
Average Capacity Loss	5.68(%)
Average Charge Ah Throughput	2491 Ah
RPT number	t0 ~ t19

Table 6. Overview of aging experiment data

IV. Results and Discussion

4.1 Determination of the degree of stress accumulation

In the configuration of the Empirical model, the term $(AhTP)^{\alpha}$ represents the degree of stress accumulation, determining the shape of the model curve as the capacity loss is decided by the increasing Ah throughput. Since the term has the form of an exponential function with an exponent less than 1, when the coefficients are the same, as the exponent increases until 1, the curve becomes closer to a straight line, as shown in Figure 10. We can see that the capacity loss curve of lithium-ion batteries is depicted in most papers [5,6,9,10] as an exponential function that is fast at the beginning and becomes slow at a certain value.

Numerous papers report that the formation of the SEI layer has a significant impact on the capacity loss of lithium-ion batteries [9,16]. It has been reported that the capacity loss due to calendar aging mode occurs according to the square root of time, that is, $\alpha=0.5$. Therefore, α is a value related to the formation of the SEI layer. In the case of this experiment combining calendar aging mode and cycling aging mode, it will have a value greater than 0.5.

In order to determine the exponent α that best fits the general shape of the aging experimental data curve, various values of f(X) were substituted for each α, and the error metrics were evaluated. The error value was found to be the lowest when α was 0.8, leading to the selection of this value as the exponent α in this study. Detailed fitting results and error metrics can be found in Table 5.

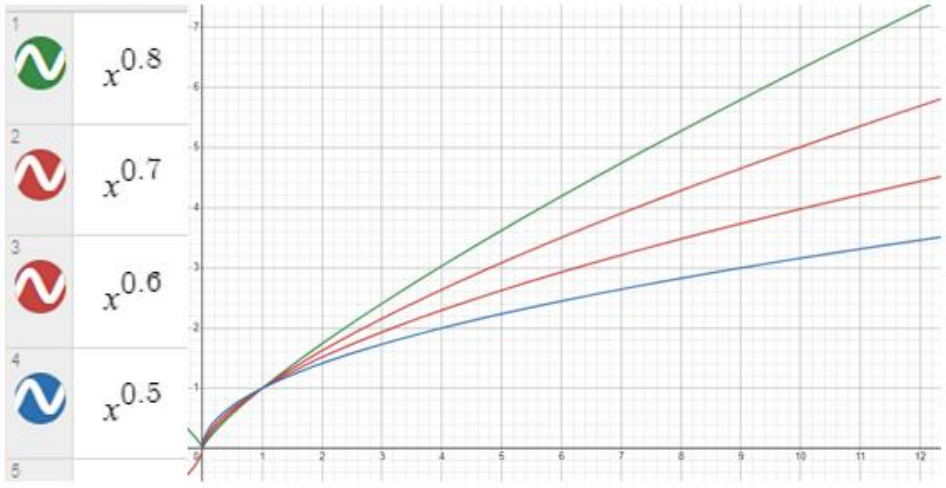

Figure 10. Changes in shape based on their exponent

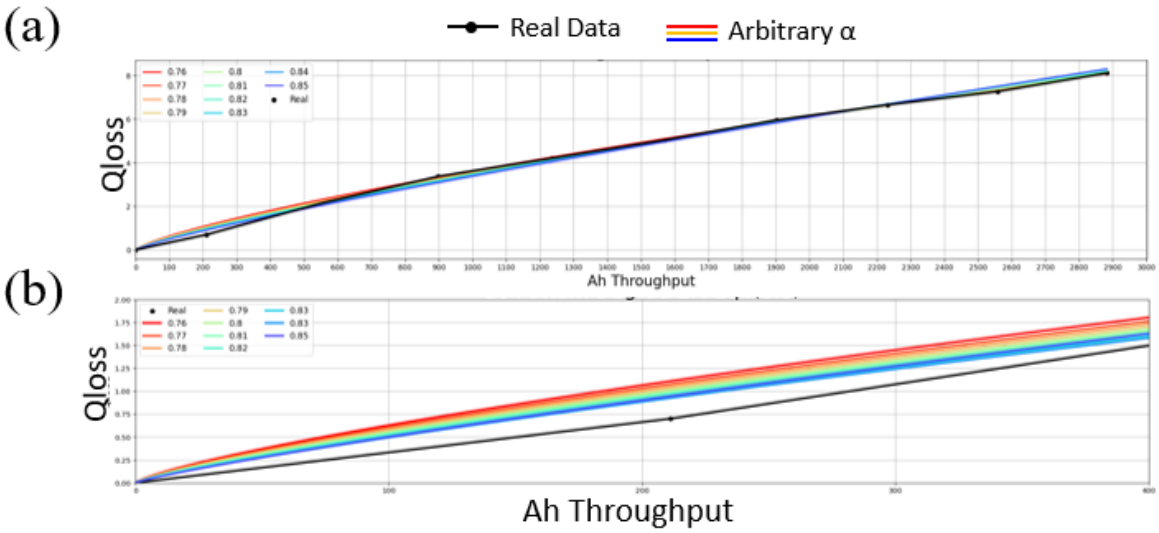

Figure 11. (a) Shape of the curve based on the α value, (b) Enlarged view of the initial part of (a)

α	f()	MAE	RMSE	R^2
0.76	0.0189	0.09116	0.14432	0.99698
0.77	0.0175	0.08396	0.13546	0.99734
0.78	0.0162	0.08143	0.12932	0.99758
0.79	0.015	0.08391	0.12628	0.99769
0.80	0.0139	0.08904	0.12633	0.99769
0.81	0.0129	0.09386	0.12971	0.99756
0.82	0.012	0.10712	0.13851	0.99722
0.83	0.0111	0.11867	0.14519	0.99694
0.84	0.0103	0.13121	0.15673	0.99644
0.85	0.0095	0.14171	0.16547	0.99603

Table 7. Fitting results with aging data based on the α value

4.2 Determination of strength of stress

In this study, charging current, discharge current, SOC and DOD were specified as stress factors. An initial quadratic polynomial representing the strength of stress was created by multiplying the stress factors with the coefficients that represent their respective influences.

Appropriate coefficient values of a polynomial were obtained using a curve-fitting method in Python. This method utilized stress factors extracted from data collected during performing an aging experiment. Figure 12 displays a plot illustrating a curve generated by substituting each stress factor and AhTP into a polynomial created through curve fitting. The capacity loss resulting from the RPT of the aging experiment represented by dots on the plots.

Since the initial polynomial is a second-order polynomial for all stress factors, it is too long and complex. Therefore, the formula needs to be optimized. The coefficients of each stress factor term represent the influence of each term on degradation. Terms with less influence on degradation can be removed by comparing their absolute values. As illustrated in Figure 13, the comparison of the absolute values of the coefficients revealed that DOD had the most significant effect on capacity loss. Several terms with extremely small values compared others were eliminated to create an optimized new formula, as depicted in Figure 14.

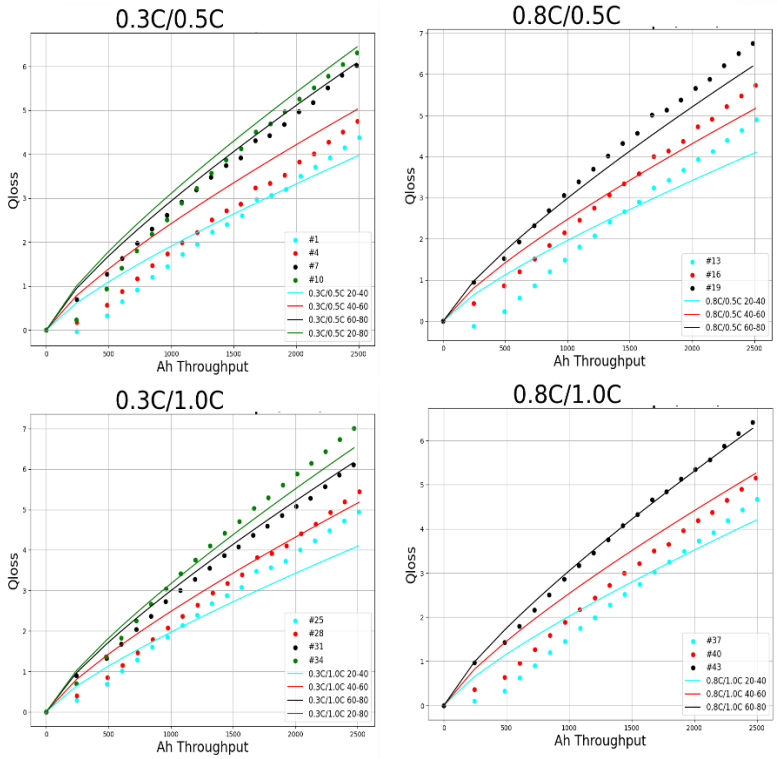

Figure 12. A plot illustrating the curve substituting stress factors and AhTP, with the RPT results of the aging experiments marked as dots

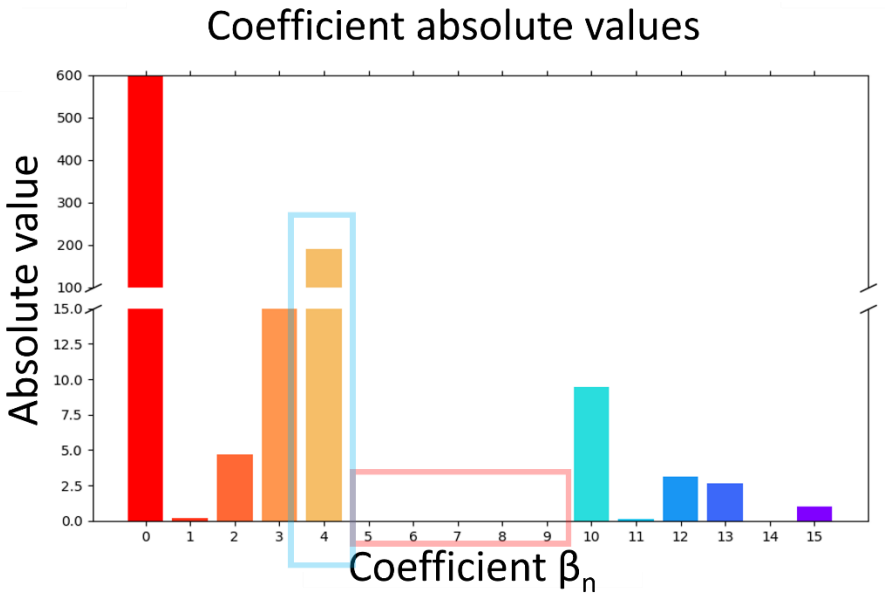

Figure 13. Results of the absolute value comparison of coefficients

$$\beta_0 + \beta_1 I_C + \beta_2 I_D + \beta_3 SoC + \beta_4 DoD + \beta_5 I_C I_D + \beta_6 I_C SoC + \beta_7 I_C DoD + \beta_8 I_D SoC + \beta_9 I_D DoD + \beta_{10} SoC \cdot DoD + \beta_{11} I_C^2 + \beta_{12} I_D^2 + \beta_{13} SoC^2 + \beta_{14} DoD^2$$

$$\beta_0 + \beta_1 I_C + \beta_2 I_D + \beta_3 SoC + \beta_4 DoD + \beta_5 SoC \cdot DoD + \beta_6 I_C^2 + \beta_7 I_D^2 + \beta_8 SoC^2$$

Figure 14. Initial polynomial and optimized new formula

4.3 Capacity loss estimation results of pattern aging data

Through processes 4.1 and 4.2, I have developed an Empirical model that can estimate the capacity loss of a degraded battery under specific conditions. To estimate the capacity loss of dynamically degraded pattern aging experiment data using this model, the operating conditions and resulting AhTP were extracted over time while tracking the degradation process of the data. These values were then substituted into the model, and the final capacity loss was estimated by connecting them using the CAP method. The red dot in Figure 15 represents the capacity loss in the RPT result of the pattern aging data, with the line following it. In the top plot, a capacity loss curve was obtained by substituting each condition extracted from the pattern aging data into the Empirical model, and the blue line shows how that the model is connected based on the degradation of the pattern aging data.

The final estimation results are displayed in the lower plot of Figure 15. The comparison between real and estimated values at each along with error metrics, is presented in Tables 6 and 7. While the estimated capacity loss indicated by the blue line is marginally lower than the actual value on average, it can be deemed successful with a low error rate of approximately 0.17% based on SOH.

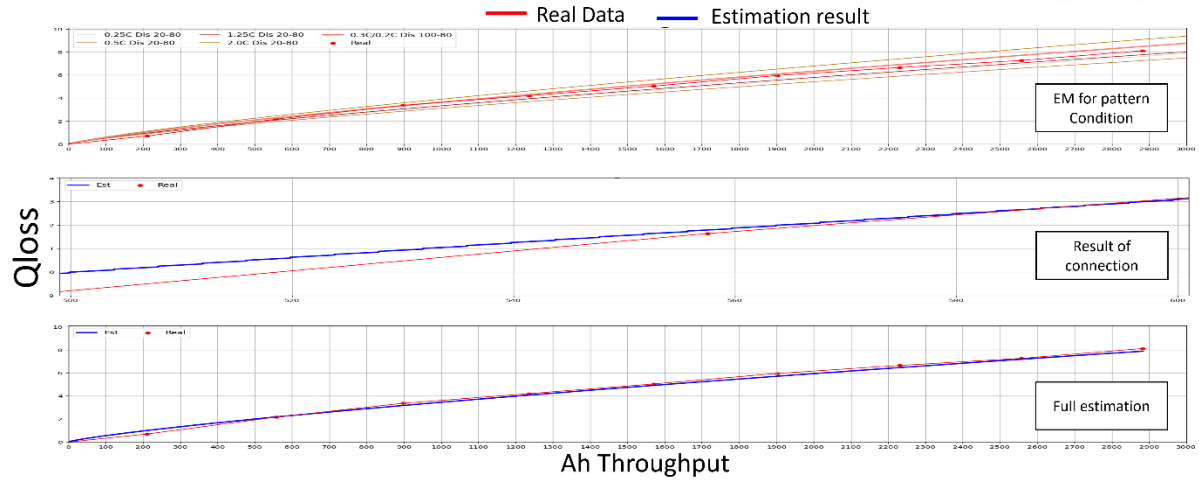

Figure 15. Plot of the result obtained by connecting models using the CAP method

Evaluation metrics	Value
MAE	0.1505
RMSE	0.1778
R^2	0.9954

Table 8. Error metrics of the estimation result

Point	Estimated Value(A)	Real Value(B)	Error(A-B)
1	98.9954	99.3005	-0.3051
2	97.8215	97.8368	-0.0153
3	96.8279	96.6336	0.1943
4	95.9248	95.7969	0.1279
5	95.0537	94.9602	0.0935
6	94.2922	94.0472	0.2450
7	93.5383	93.3508	0.1875
8	92.8164	92.7380	0.0784
9	92.1190	91.8903	0.2287
Average(Abs)			0.1639

Table 9. Results of comparing real and estimated values at nine points of pattern aging data

4.4 Capacity loss estimation in dynamic DOD changing patterns

The previous pattern degradation data aged repeatedly within a specific DOD range (SOC 20%-80%). It was evaluated that there was a deficiency in replicating the behavior of the actual EV battery. To address this issue, I collected data that had been aged with varying DOD levels across for all possible cases within the range. I then estimated the capacity loss of the data to assess its ability to replicate the behavior of the actual EV battery. Figure 16 displays a plot comparing the previous pattern aging data with the new pattern, while Table 8 presents the total number of cases with variable DODs used in the new aging pattern.

As a result, even though the experimental period was brief and a small number of data points were compared, the error remained similarly low as before. This confirmed the model's ability to accurately estimate the behavior of actual EV batteries. Tables 9 and 10 display error metrics and value comparisons from additional experiments, similar to the scenario in section 4.3.

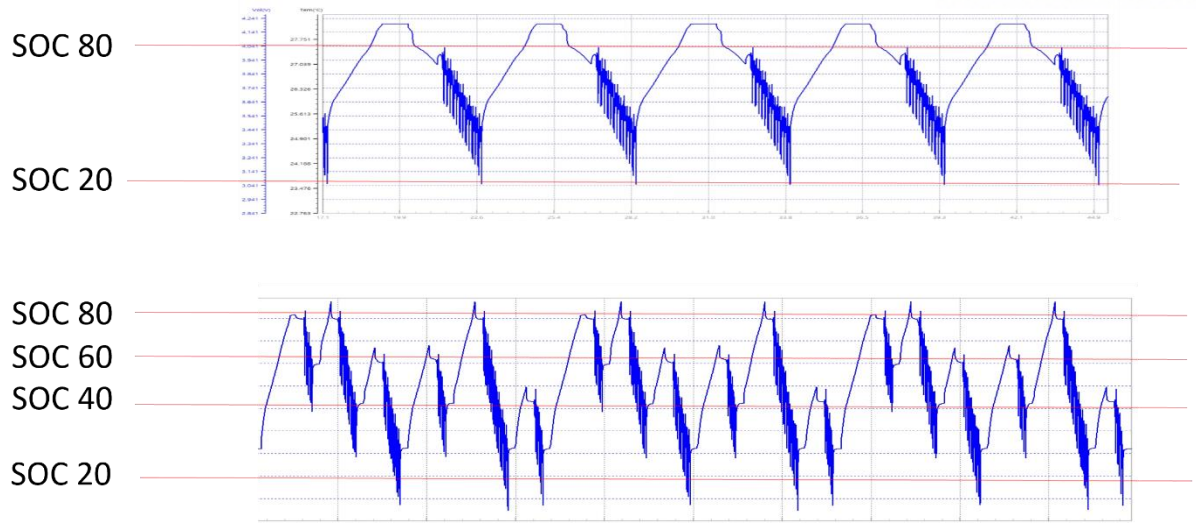

Figure 16. Previous aging pattern with a constant DOD and the new aging pattern with a variable DOD

Case	Charge	Discharge	DOD
1	20->80	80->20	60
2	20->60	60->20	40
3	40->80	80->40	40
4	20->40	40->20	20
5	40->60	60->40	20
6	60->80	80->60	20

Table 10. Number of cases for variable DODs used in the new aging pattern

Evaluation metrics	Value
MAE	0.0734
RMSE	0.1041
R^2	0.9662

Table 11. Error metrics of the estimation results for the new aging pattern

Point	Estimated Value(A)	Real Value(B)	Error(A-B)
1	99.3254	99.3616	-0.0362
2	98.8312	98.8933	-0.0621
3	98.2794	98.4748	-0.1954
Average(Abs)			0.0979

Table 12. Results of comparing real and estimated values of the new aging pattern

V. Conclusion

The significance of this study lies in the development of a method that combines the Empirical model and the CAP method. This method is expressed in the form of the stress factor and connects models established under different operating conditions. It can estimate the SOH with high accuracy by substituting the stress factor extracted from pattern aging data, even with a small amount of computational power. However, the experiments were only conducted in the linear degradation section above 80% SOH. Therefore, further studies are needed to estimate the nonlinear degradation section where rapid capacity loss occurs. Additionally, the effect of temperature was excluded due to the limitations of the experimental environment.

Currently, development is underway on equipment, including OBD readers, which enable data extraction from EVs. The extracted data change much more rapidly and are more complex compared to the pattern aging data used in this study. Therefore, we will also need to develop technologies that convert it into patterned data that can be easily analyzed. If this technology and the method developed in this study are combined, it is expected that cost-effective onboard SOH estimation in EVs will be possible. Furthermore, it could also enable the recommendation of optimized driving patterns to users that can use the battery more efficiently.

In conclusion, this study can be evaluated as not only laying the foundation for a technology that can estimate SOH in real time despite the insufficient computational power of EVs, but also establishing the groundwork for a commercial aspect that can offer state diagnosis services for EV batteries under various operating conditions.

VI. Reference

[1] IEA (2023), Lithium-ion battery manufacturing capacity, 2022-2030, IEA, Paris https://www.iea.org/data-and-statistics/charts/lithium-ion-battery-manufacturing-capacity-2022-2030

[2] The New York Times (2022), Apple Becomes First Company to Hit $3 Trillion Market Value, https://www.nytimes.com/2022/01/03/technology/apple-3-trillion-market-value.html

[3] König, A.; Nicoletti, L.; Schröder, D.; Wolff, S.; Waclaw, A. & Lienkamp, M. (2021). An Overview of Parameter and Cost for Battery Electric Vehicles, World Electric Vehicle Journal, 12, 21. https://doi.org/10.3390/wevj12010021

[4] Birkl, C. R.; Roberts, M. R.; McTurk, E.; Bruce, P. G. & Howey. D. A. (2017). Degradation diagnostics for lithium ion cells. Journal of Power Sources, 341, 373-386. https://doi.org/10.1016/j.jpowsour.2016.12.011

[5] Ploehn, H. J.; Ramadass, P. & White, R. E. (2004). Solvent Diffusion Model for Aging of Lithium-Ion Battery Cells. Journal of The Electrochemical Society, 151(3), A456-A462. https://doi.org/10.1149/1.1644601

[6] Broussely, M.; Herreyre, S.; Biensan, P.; Kasztejna, P.; Nechev, K. & Staniewicz, R. J. (2001). Aging mechanism in Li ion cells and calendar life predictions. Journal of Power Source, vol. 97-98, 12-21. https://doi.org/10.1016/S0378-7753(01)00722-4

[7] Alyakhni, A; Boulon, L.; Vinassa, J. M. & Briat, O. (2021). A Comprehensive Review on Energy Management Strategies for Electric Vehicles Considering Degradation Using Aging Models. IEEE Access, vol. 9, 143922-143940. https://doi.org/10.1109/ACCESS.2021.3120563

[8] Meng, J.; Luo, G.; Ricco, M.; Swierczynski, M.; Stroe, D. I. & Teodorescu, R. (2018). Overview of Lithium-Ion Battery Modeling Methods for State-of-Charge Estimation in Electrical Vehicles. Applied Science, 8, 659. https://doi.org/10.3390/app8050659

[9] Mathieu, R.; Baghdadi, I.; Briat, O.; Gyan, P. & Vinassa, J. M. (2017) D-optimal design of experiments applied to lithium battery for ageing model calibration. Energy, 141, 2108-2119. https://doi.org/10.1016/j.energy.2017.11.130

[10] Karger, A.; Wildfeuer, L.; Aygül, D.; Maheshwari, A.; Singer, J. P. & Jossen, A. (2022) Modeling capacity fade of lithium-ion batteries during dynamic cycling considering path dependence. Journal of Energy Storage, vol. 52, 104718. https://doi.org/10.1016/j.est.2022.104718

[11] Preger, Y.; Barkholtz, H. M.; Fresquez, A.; Campbell, D. L.; Juba, B. W.; Romàn-Kustas, J.; Ferreira, S. R. & Chalamala, B. (2020) Degradation of Commercial Lithium-Ion Cells as a Function of Chemistry and Cycling Conditions. Journal of The Electrochemical Society, 167, 120532. https://doi.org/10.1149/1945-7111/abae37

[12] Park, K. J.; Hwang, J. Y.; Ryu, H. H.; Maglia, F.; Kim, S. J.; Lamp, P.; Yoon, C. S. & Sun, Y. K. (2019) Degradation Mechanism of Ni-Enriched NCA Cathode for Lithium Batteries: Are Microcracks Really Critical?. ACS Energy Letters, 4, 6, 1394-1400. https://doi.org/10.1021/acsenergylett.9b00733

[13] ISO (2012), ISO 12405-2 Electrically propelled road vehicles — Test specification for lithium-

ion traction battery packs and systems, Part 2: High-energy applications. https://www.iso.org/standard/55854.html

[14] Su, L.; Zhang, J.; Huang, J.; Ge, H.; Li, Z.; Xie, F. & Liaw, B. Y. (2016). Path dependence of lithium ion cells aging under storage conditions. Journal of Power Source, vol. 315, 35-46. http://dx.doi.org/10.1016/j.jpowsour.2016.03.043

[15] Werner, D.; Paarmann, S. & Wetzel, T. (2021). Calendar Aging of Li-Ion Cells-Experimental Investigation and Empirical Correlation. Batteries, 7(2), 28. https://doi.org/10.3390/batteries7020028

[16] Schmalstieg, J.; Käbitz, S.; Ecker, M. & Sauer, D. U. (2014). A holistic aging model for Li(NiMnCo)O2 based 18650 lithium-ion batteries. Journal of Power Source, 257, 325-334. https://doi.org/10.1016/j.jpowsour.2014.02.012

Acknowledgments

First of all, I would like to express my endless gratitude to my advisor, Professor Yunseok Choi. I would like to take this opportunity to once again express my gratitude to my advisor, who generously gave me advice, sometimes strictly and sometimes kindly, and always guided me in the direction of my research during difficult times.

I would also like to express my sincere gratitude to the two professors, Professor Youngsik Kim and Wang-Geun Lee, who readily agreed to be appointed as committee members for my master's thesis. Thanks to these two professors, I was able to successfully complete my master's program and move on to a promising future.

I cannot leave out my gratitude to our lab members. Our team leader, Junwoo Bae, always provided advice and encouragement. Dawoon Jung, who was actually an older brother, but he supported me a lot like a friend, Taeyoung Kim, who helped me with his wealth of knowledge, Soobin Park, life of the party in our lab, is now working for conglomerate company SK, and Raehyoung Yoo & Sanghyeok Park, who will step into my shoes in the master's program in our lab next semester. I would like to express my sincere gratitude to all the lab members, regardless of the amount of help.

Special thanks are extended to Better Life Battery (BLB) Corp for generously providing financial support, enabling me to conduct fruitful research without any difficulty.

Lastly, I would like to thank my parents for believing in me and supporting me to make all of this possible.